

OB-stars as extreme condition test beds

Joachim Puls¹, Jon O. Sundqvist¹ and Jorge G. Rivero González¹

¹ Universitätssternwarte der Ludwig-Maximilians-Universität München
Scheinerstr. 1, D-81679 München, Germany
email: uh101aw@usm.uni-muenchen.de (J.P.)

Abstract. Massive stars are inherently extreme objects, in terms of radiation, mass loss, rotation, and sometimes also magnetic fields. Concentrating on a (personally biased) subset of processes related to pulsations, rapid rotation and its interplay with mass-loss, and the bi-stability mechanism, we will discuss how active (and normal) OB stars can serve as appropriate laboratories to provide further clues.

Keywords. hydrodynamics, instabilities, line: formation, stars: abundances, stars: early-type, stars: evolution, stars: mass loss, stars: oscillations, stars: rotation, stars: winds, outflows

1. Introduction

Massive stars are inherently extreme objects, in terms of radiation, mass loss, rotation and sometimes also magnetic fields. Thus, they can serve as test beds for extreme conditions and corresponding theoretical predictions. Such tests are, e.g., particularly important for our understanding of the (very massive) First Stars and for the physics of fast rotation in massive stars, which is a key ingredient in the collapsar model of long Gamma Ray Bursts. In this review we discuss how a variety of physical processes present in massive stars can affect both their stellar photospheres and/or winds, and how active (and normal) OB stars can be, and are, used as appropriate laboratories to provide further clues. In the following, we concentrate on a (personally biased) subset of processes related to pulsations (Sect. 2), rapid rotation and its interplay with mass-loss (Sect. 3), and mass-loss itself, particularly on the bi-stability mechanism (Sect. 4).

2. Pulsations

2.1. Pulsating B-supergiants

Well outside the instability strips of β Cep and slowly pulsating B-stars (SPB), Waelkens *et al.* (1998) via HIPPARCOS detected 29 periodically variable B-supergiants. A corresponding instability region had not been predicted at that time. Meanwhile, however, Pamyatnykh (1999) and Saio *et al.* (2006, see also this volume) identified such regions for pre-TAMS and post-TAMS objects, respectively, with SPB-type of oscillations (high order g-modes). These regions are indicated in Fig. 1, together with results from quantitative spectroscopy by Lefever *et al.* (2007), for those of the above 29 supergiants with sufficient spectral information. Obviously, most of these objects are located very close to the high gravity limit of the predicted pre-TAMS or within the predicted post-TAMS instability strips for evolved stars. Together with their multi-periodic behaviour, this strongly suggests that these objects are opacity-driven non-radial pulsators (NRPs), and thus are ideal **test beds** for asteroseismologic studies of evolved massive stars. Note that Lefever *et al.* (2007) found additional periodically variable objects not known to be pulsators so far, and suggested, from their pulsational behaviour and their positions, that these objects are g-mode pulsators as well. Two of them, HD 64760 (B0.5 Ib) and

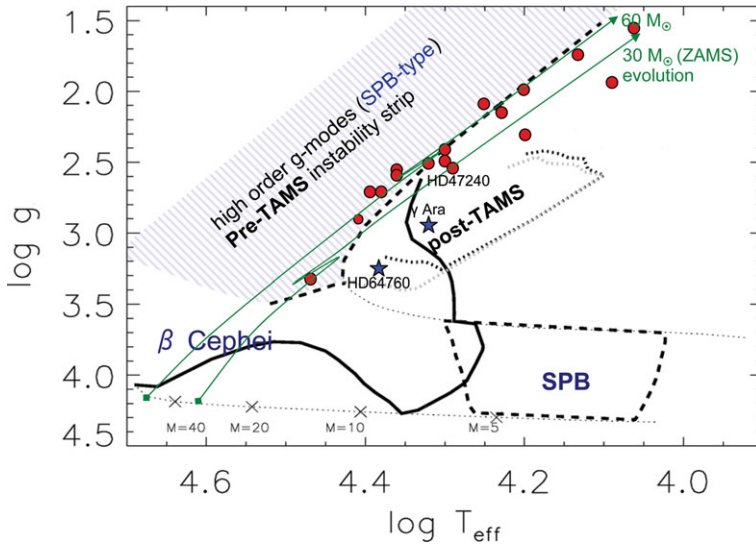


Figure 1. $\log T_{\text{eff}}\text{-}\log g$ diagram for hot massive stars. Indicated are the instability regions for β Cep stars (solid bold), SPBs close to the ZAMS (dashed bold) and SPBs of evolved type as predicted by Pamyatnykh (1999) (pre-TAMS, blue hatched) and Saio *et al.* (2006) (post-TAMS, dotted). Red dots correspond to the positions of slowly pulsating B-supergiants from the sample by Waelkens *et al.* (1998) as derived by Lefever *et al.* (2007), and blue asterisks are two newly suggested g-mode pulsators from the same work. See text for further details. Adapted from Lefever *et al.* (2007).

γ Ara (= HD 157246, B1 Ib), are explicitly indicated in Fig. 1, together with HD 47240 (B1 Ib) from the original sample by Waelkens *et al.*, and will be referred to later on.

2.2. Macroturbulence

A present key problem in atmospheric diagnostics by high resolution spectroscopy is the finding that the line-profiles from (at least) late O- and B-supergiants display substantial extra-broadening (in addition to the well-known effects from rotation etc.), which has been termed ‘macro-turbulence’ (for details and references, see Simón-Díaz *et al.* 2010). This extra-broadening can be simulated by allowing for a *supersonic* Gaussian or quasi-Gaussian velocity distribution in photospheric regions, which is difficult to justify physically. Recently, however, Aerts *et al.* (2009) showed that such extra-broadening can be reproduced from the *collective* effect of low-amplitude g-mode oscillations. First hints that this scenario might be realistic have been found by Simón-Díaz *et al.* (2010), from a tight observed correlation between the peak-to-peak amplitudes of velocity moments measured from (variable) photospheric profiles of B-supergiants and the derived macro-turbulent broadening. Given the ubiquity of macro-turbulence in hot massive stars, this tentatively suggests that a large fraction of OB-stars are non-radial pulsators (see also Fullerton, this volume).

2.3. Triggering of structure/clump formation

With respect to their stellar winds, pulsations in massive stars might be responsible for inducing large-scale structures, such as co-rotating interaction regions (CIRs, see Fullerton, this volume), and, particularly, for triggering the formation of clumps: To reproduce the observed X-ray emission from hot stellar winds, $L_x \approx 10^{-7} L_{\text{bol}}$, the line-driven (or deshadowing) instability related to radiative line driving needs to be excited by deep-seated photospheric disturbances of a multitude of frequencies (NRPs?), giving

rise to strong clump-clump collisions and consequently strong shocks (Feldmeier *et al.* 1997a,b). For models with self-excited instability alone, the predicted X-ray emission is much too weak. Moreover, such perturbations might be responsible for triggering the on-set of *deep-seated* wind-clumping (Sect. 4), as implied from various diagnostics (e.g., Bouret *et al.* 2005; Puls *et al.* 2006; Sundqvist *et al.* 2011).

2.4. Strange mode oscillations

In addition to ‘conventional’ pulsations, another class of quasi-periodic, *dynamical* instabilities are predicted to occur in the envelopes of luminous stars with large $L/M > 10^3$. These are the so-called strange-mode oscillations (for details and references, see Saio and Chené, this volume), which should be particularly strong in WR-stars and might even help to initiate their winds (e.g., Wende *et al.* 2008). So far, there is no direct evidence of these predictions, though the strongest amplitudes of optical lrv in O-stars are located within the region of predicted strange mode oscillations (Fullerton *et al.* 1996), and at least for one WR star such oscillations might actually have been observed (see Chené, this volume). Alternative **test beds** to check the reality of strange mode oscillations might be late B-/early A-supergiants (as suggested by Puls, Glatzel, & Aerts as targets for the micro-satellite BRITe), since, in comparison to WRs, these objects have less dense winds and ‘convenient’ frequencies (on the order of a few to tens of days), with predicted amplitudes of 0.1 mag (W. Glatzel, priv. comm.). Indeed, the COROT observations of the late B-supergiant HD 50064 (Aerts *et al.* 2010) showed a period of 37 days, with a sudden amplitude change by a factor of 1.6. Together with other evidence (variable \dot{M} etc.), Aerts *et al.* tentatively interpreted this finding as the result of a strange mode oscillation.

3. Rapid rotation

3.1. Photospheric deformation and gravity darkening

Rapid rotation affects the stellar photosphere in (at least) two ways. First, it becomes deformed, with $R_{\text{eq}}/R_{\text{pole}} = 1.5$ at critical rotation (using a Roche model with point mass distribution, see Zhao, this volume, and Cranmer & Owocki 1995 for details and references). The first observational **test bed** which confirmed the basic effect was the brightest Be star known, Achernar = α Eri (VLTI observations by Domiciano de Souza *et al.* 2003).

The second effect is gravity darkening, first suggested by von Zeipel (1924), who assumed rotational laws that can be derived from a potential, e.g., uniform or cylindrical. An important extension was provided by Maeder (1999), who considered the more realistic case of shellular rotation in radiative envelopes, where the angular velocity is assumed to be constant on horizontal surfaces (Zahn 1992). In result, the photospheric flux is proportional to the *effective* gravity, $\vec{F} \propto \vec{g}_{\text{eff}}(1 + \zeta(\vartheta))$, with $|\zeta(\vartheta)| < 0.1$ in most cases and $\zeta = 0$ in the original von Zeipel case. The effective gravity is the vector sum of gravitational and centrifugal acceleration, $\vec{g}_{\text{eff}} = \vec{g}_{\text{grav}} + \vec{g}_{\text{cent}}$, i.e., lower at the equator than at the pole, with $\vec{g}_{\text{eff}}(\text{pole}) = \vec{g}_{\text{grav}}$. Note that here \vec{g}_{eff} is *independent of the radiative acceleration!* Neglecting $\zeta(\vartheta)$, for radiative envelopes we obtain $T_{\text{eff}}(\vartheta) \propto g_{\text{eff},\perp}^{1/4}$, i.e., T_{eff} decreases towards the equator, in dependence of the normal component of \vec{g}_{eff} .

Both effects are demonstrated in Fig. 2, for a typical O-supergiant rotating close and very close to critical rotation. Deformation and gravity darkening become significant only for rotational speeds higher than roughly 70% of the critical one! **Test beds** to check

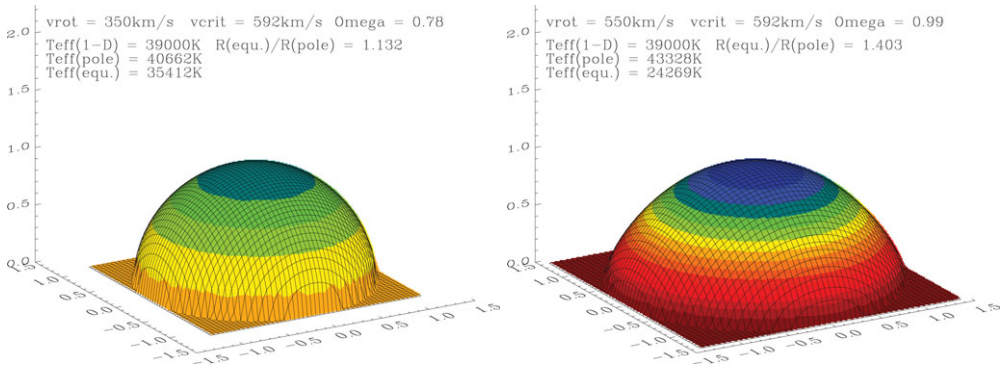


Figure 2. Predicted photospheric deformation and gravity darkening for a star similar to ζ Pup (1-D values: $T_{\text{eff}}=39$ kK, $R_{*}=19R_{\odot}$, $\log g=3.6$) but rotating with 78% (left) and 99% (right) of its critical angular velocity. Both figures are on the same scale, with identical color coding for $T_{\text{eff}}(\vartheta)$. The ratios $R_{\text{eq}}/R_{\text{pole}}$ and the effective temperatures at the hotter pole and cooler equator are indicated within the figures.

both effects are discussed by Zhao (this volume; see also the summary provided by van Belle 2010).

3.2. Rapid rotation and winds

Standard line-driven wind theory (for a recent review and references, see Puls *et al.* 2008) predicts that the mass-loss rate of a non (slowly) rotating star scales as

$$\dot{M} \propto (N_{\text{eff}} L)^{1/\alpha} (g_{\text{grav}} R_{*}^2 (1 - \Gamma))^{1-1/\alpha},$$

with N_{eff} the effective number of driving lines (proportional to the force-multiplier parameter k , Castor *et al.* 1975, CAK), CAK parameter α (corresponding to the steepness of the line-strength distribution function), and Eddington factor Γ . Accounting for rotation (and Γ not too large), we find that the mass-loss rate depends on co-latitude θ ,

$$\begin{aligned} \dot{M}(\theta) &\propto (N_{\text{eff}}(\theta) F(\theta) R_{*}^2(\theta))^{1/\alpha(\theta)} (g_{\text{eff}}(\theta) R_{*}^2(\theta) (1 - \Gamma))^{1-1/\alpha(\theta)} \\ &\underset{\text{von Zeipel}}{\propto} (N_{\text{eff}}(\theta))^{1/\alpha(\theta)} g_{\text{eff}}(\theta) R_{*}^2(\theta) \end{aligned} \quad (3.1)$$

(cf. Owocki *et al.* 1998). This expression renders two possibilities. i) If the ionization equilibrium is rather constant w.r.t. θ (as it is the case for O-stars), we obtain a *prolate* wind structure, since $g_{\text{eff}}(\theta)$ is largest at the pole. This is the g_{eff} -effect, see Owocki *et al.* (1998); Maeder (1999); Maeder & Meynet (2000). ii) If, on the other hand, the ionization equilibrium were strongly dependent on θ , this would imply an *oblate* wind structure if the increase of N_{eff} and the decrease of α towards the equator (as a consequence of decreasing ionization) could overcompensate the decrease of g_{eff} . Such a situation (the κ -effect, see Maeder 1999; Maeder & Meynet 2000) *might* occur in B-supergiants (but see Sect. 4). Note, however, that *no* thin disk can be formed by this process alone. Note also that self-consistent 2-D hydro/NLTE calculations (though somewhat simplified) for rapidly rotating B-stars around $T_{\text{eff}}=20$ kK (i.e., just in the region where the κ effect might be expected) by Petrenz & Puls (2000) still resulted in a prolate wind structure, since the ionization effects turned out to be only moderate.

Of course, these predictions need to be checked observationally, particularly when considering their importance regarding stellar evolution (e.g., a pronounced polar mass loss would lead to less loss of angular momentum), and with respect to mass-loss

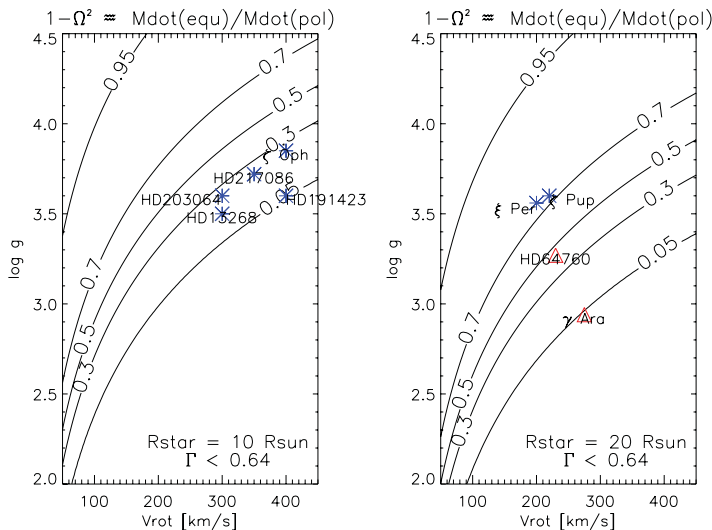


Figure 3. Iso-contours of $1 - \Omega^2 \approx \dot{M}(\text{eq})/\dot{M}(\text{pole})$ as a function of v_{rot} and $\log g$, for typical dwarfs (left) and supergiants (right). Overplotted are the positions of some rapidly rotating Galactic O-stars (asterisks) and B-supergiants (triangles), assuming a minimum $v_{\text{rot}} = v \sin i$.

diagnostics (when do we need 2-D models?). To our knowledge, clear observational evidence for aspherical winds is still missing.† So, what are potential **test beds**?

In Fig. 3 we have plotted theoretical iso-contours of $1 - \Omega^2 \approx \dot{M}(\text{eq})/\dot{M}(\text{pole})$ (from Eq. 3.1 and assuming N_{eff} and α to be constant; $g_{\text{eff}} \approx g_{\text{grav}}(1 - \Omega^2)$ and $\Omega = \omega/\omega_{\text{crit}}$) as a function of v_{rot} and $\log g$, for typical dwarfs (left) and supergiants (right). Overplotted are the locations of well-known Galactic rapid rotators, for a minimum value of $v_{\text{rot}} = v \sin i$ (data from Repolust *et al.* 2004 and Lefever *et al.* 2007). Asterisks denote O-stars, triangles B-supergiants. All O-dwarfs/giants (left) are predicted to have a significant mass-loss contrast, below 0.3. Unfortunately, their (average) mass-loss rate is too low to lead to substantial effects in the optical wind-lines and the IR continuum, though UV-spectra should be affected by deviations from spherical symmetry. For the fast rotating O-supergiants, on the other hand, the predicted effect is rather small, so nothing might be visible. Vink *et al.* (2009), using linear H_{α} spectro-polarimetry, conclude that most winds from rapidly rotating O-stars are spherically symmetric. For the two rapidly rotating B-supergiants, HD 64760 and particularly γ Ara, the situation is more promising, and they might be used as **test beds** to check the impact of rotation on the global wind topology. Remember that HD 64760 (see also Sect. 2) is one of the best studied objects in the UV (thanks to the IUE mega-campaign, Massa *et al.* 1995) - with the detection of CIRs and ‘PAMS’ (see Fullerton, this volume), both presumably related to its non-radial pulsations -, and has also been studied in the optical to clarify the interaction between NRPs and CIRs (Kaufer *et al.* 2006).

Fig. 4 (left) displays the corresponding H_{α} line profiles, for the above two rapidly rotating B-supergiants and for HD 47240 (see also Sect. 2), with a somewhat lower $v \sin i$. At first glance, these profiles might indicate the presence of a disk or an oblate wind (e.g.,

† The polar wind structures claimed for the Be-stars Achernar (Kervella & Domiciano de Souza 2006) and α Ara (Meilland *et al.* 2007) from NIR interferometry still need to be confirmed, given that - as discussed during this conference - for such low mass-loss rates the IR-photosphere is very close to the optical one (in other words, the IR-excess from the wind is very low).

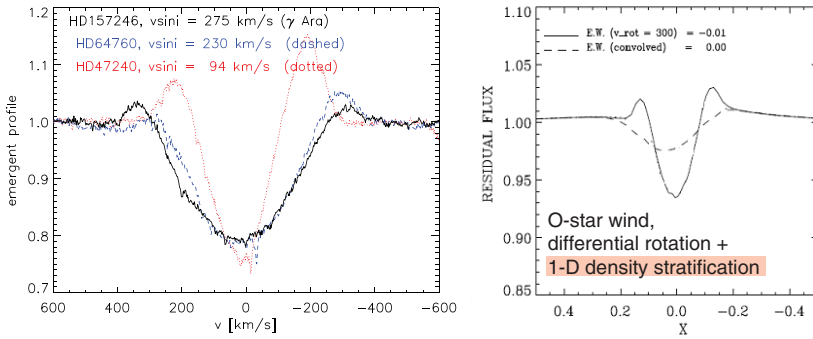


Figure 4. Left: H α line profiles for three rapidly rotating B-supergiants (spectra and data from Lefever *et al.* 2007). Right: Theoretical H α line profiles, for an O-star wind with *spherical* density stratification. Dashed: Profile convolved with a rotation profile of width 300 km s $^{-1}$. Solid: 2-D line transfer allowing for differential rotation, $v_{\text{rot}} \propto 1/r$. Adapted from Petrenz & Puls (1996).

the κ -effect from above), but this is not necessarily the case. As shown in Fig. 4 (right), even a *spherical* wind can give rise to double-peaked profiles, when accounting for the wind’s differential rotation (due to the so-called resonance-zone effect, Petrenz & Puls 1996). Note that in this case the profile only depends on the product $v \sin i$ and not on the individual factors. For a 2-D density stratification, however, the profiles will look different for a prolate or oblate topology, and will depend on the individual values of v_{rot} and $\sin i$ as well, which might induce a certain dichotomy. Interestingly, UV spectroscopy (via IUE) of γ Ara by Prinja *et al.* (1997) gave indications for a *prolate* geometry, mainly because of missing or weak emission peaks in the P Cygni profiles.

3.3. The $\Omega\Gamma$ limit

An interesting question is what happens if a star is rapidly rotating *and* close to the Eddington limit. After a controversial discussion (Langer *et al.* 1997; Glatzel 1998), Maeder & Meynet (2000) were able to solve this problem in an elegant way. For the following discussion, it is only important to note that the *total* acceleration due to gravity, centrifugal forces, and radiation pressure gradients can be expressed as $g_{\text{tot}} = g_{\text{eff}}(1 - \Gamma_{\Omega})$, where the effective gravity remains defined as previously, and $\Gamma_{\Omega}/\Gamma > 1$ is a function of $v_{\text{rot}}/v_{\text{crit}}$. Consequently, the total acceleration can become zero before the nominal Eddington limit is reached, and this new limit is called the $\Omega\Gamma$ limit. As shown by Maeder & Meynet (2000), the combination of rapid rotation and large Γ can affect the total (polar-angle integrated) mass-loss rate from a radiation driven wind considerably,

$$\frac{\dot{M}(\text{rotating})}{\dot{M}(\text{non-rotating})} \approx \left(\frac{1 - \Gamma}{\Gamma/\Gamma_{\Omega} - \Gamma} \right)^{\frac{1}{\alpha} - 1} \begin{cases} = O(1) & \text{for not too fast rotation and low } \Gamma \\ \gg 1 & \text{for fast rotation and considerable } \Gamma \\ \text{but:} & \text{max. } \dot{M} \text{ limited because } L \text{ limited} \end{cases}$$

since α is on the order of 0.4 ... 0.6. To identify potential **test beds** to check this important prediction, in Fig. 5 we have plotted the iso-contours of the v_{rot} required for a significantly increased mass-loss rate, as a function of T_{eff} and $\log g$. (A factor of four compared to the non-rotating case was chosen to allow for an easy observational check.) The red shaded region comprises the approximate locations of Galactic OB-supergiants. Overplotted are the positions of some rapidly rotating supergiants, O-types (asterisks) and B-types (triangles). The numbers in brackets are the observed $v \sin i$. Again, O-supergiants are not suited as test beds, since they would need to rotate much faster than

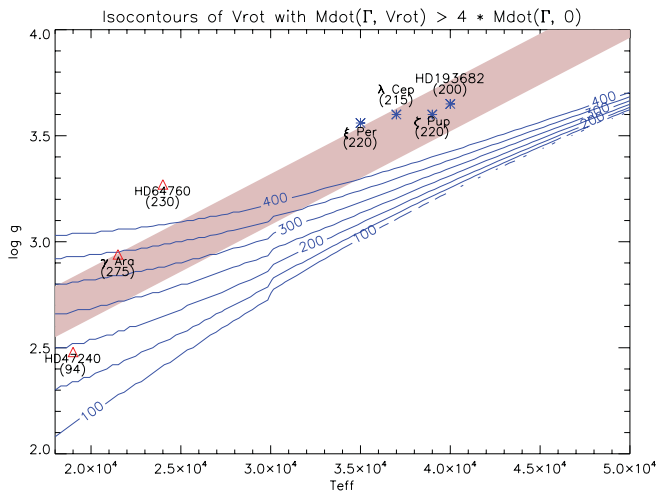


Figure 5. Iso-contours of v_{rot} for which the total mass-loss rate is predicted to become increased by a factor of four, compared to the non-rotating case, as a function of T_{eff} and $\log g$, together with the positions and $v \sin i$ -values of some rapidly rotating O- and B-supergiants (asterisks and triangles, respectively). See text.

400 km s^{-1} to show the required increase in \dot{M} . Interestingly, however, at least γ Ara (and maybe HD 47240 - if its $\sin i$ were 0.5) are located at the ‘right’ position and might be worth being investigated in detail, e.g., by means of interferometry (see Chesneau, this volume) in combination with 2-D NLTE modeling (Georgiev *et al.* 2006). The outcome of such investigations will be of particular relevance for stellar evolution with rapid rotation, especially in the early Universe (see Ekström, this volume).

4. Mass loss

As we have seen, rapidly rotating B-supergiants are ideal **test beds** to check a number of theoretical predictions. Unfortunately, however, there exists only few such objects, since there is a rapid drop of rotation below $T_{\text{eff}} \approx 20 \text{ kK}$, as is obvious from the distribution of $v \sin i$ (e.g., Howarth *et al.* 1997). In a recent letter, Vink *et al.* (2010) tried to explain this finding based on two alternative scenarios (see also Langer, this volume). In *scenario I*, the low rotation rates of B-supergiants are suggested to be caused by braking due to an increased mass loss for $T_{\text{eff}} < 25 \text{ kK}$, where this increased mass loss should be due to the so-called bi-stability jump. Vink *et al.* termed this process ‘bi-stability braking’.

4.1. The bi-stability jump

The bi-stability jump itself has often been discussed and referred to in the literature, and goes back to findings by Pauldrach & Puls (1990) when modeling the wind of P Cygni. These findings were generalized by Vink *et al.* (2000, 2001) in their work on stellar wind models for OB-stars: In the intermediate/late O-star and early B-star regime, the major contribution of driving lines in the lower wind (which are responsible for initiating the mass-loss rate) is from Fe IV. Below $T_{\text{eff}} = 23 \text{ kK}$, however, Fe IV recombines more or less abruptly to Fe III. Since Fe III has more effective lines than Fe IV, N_{eff} increases (in parallel with a decrease of α , see also Puls *et al.* 2000), which leads to an increase in \dot{M} and a decrease in the terminal velocity, v_{∞} . This is the theoretical basis for the κ -effect discussed in Sect. 2. Vink *et al.* (2000) predict a typical increase in \dot{M} by a factor of

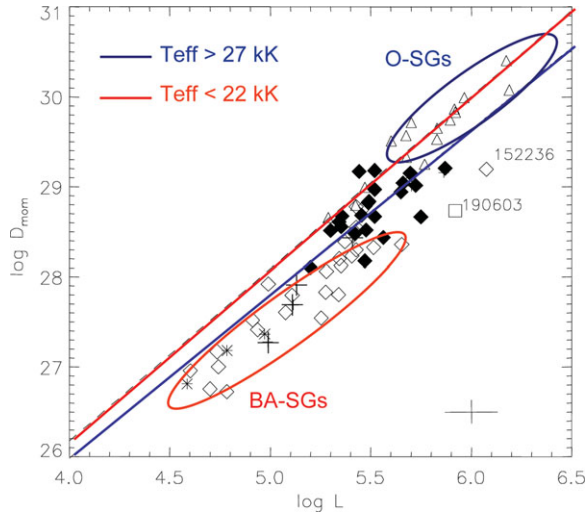


Figure 6. Modified wind-momenta for Galactic O- and B-supergiants. Dashed (red) and solid (blue) lines represent the predictions by Vink *et al.* (2000) for objects below and above 23 kK, respectively. Triangles are O-supergiants ($T_{\text{eff}} > 27$ kK), filled diamonds early B-sgs with $T_{\text{eff}} > 22$ kK and open triangles B-supergiants below this value. The cross in the lower right displays the typical error bars. Adapted from Markova & Puls (2008).

five, and a decrease in v_{∞} by a factor of two. Consequently, the wind-momenta from massive stars with $T_{\text{eff}} < 23$ kK should be *higher* than those from stars of earlier spectral types (see dashed/solid lines in Fig. 6.) This important prediction needs to be checked observationally, not least because present day evolutionary codes often incorporate the corresponding ‘mass-loss recipe’.

4.2. Test beds for the bi-stability jump (I): B[e]-supergiants?

The hybrid spectrum of B[e] supergiants can be explained by a two-component wind, with an outflowing ‘disk’ (equatorial wind) of low velocity, high density and low ionization, and a high velocity, low density and highly ionized polar wind (Zickgraf *et al.* 1986, 1989). A first explanation of this wind structure was given by Lamers & Pauldrach (1991), who combined the effects of fast rotation and bi-stability jump, following the calculations from Pauldrach & Puls (1990) for the latter: The high values of g_{eff} together with the high ionization at the pole (T_{eff} calculated via von Zeipel) then give rise to a fast and thin polar wind, whereas the low $g_{\text{eff}}/T_{\text{eff}}$ values at the equator induce a slow and dense wind. (Note that v_{∞} scales with the photospheric escape velocity and thus with g_{eff} , see below).

Until now, the B[e]-sg mechanism is heavily debated. Owocki *et al.* (1998) pointed out that Lamers & Pauldrach (1991), though accounting for gravity darkening when calculating the ionization, did not include its impact on \dot{M} (Eq. 3.1). When gravity darkening is included into the accelerating flux, $F(\theta) \propto g_{\text{eff}}(\theta)$, a ‘disk’ formation becomes almost impossible, due to the counteracting effects of bi-stability and increased polar flux (see also Puls *et al.* 2008 and references therein). Simulations by Pelupessy *et al.* (2000), on the other hand, indicated that the bi-stability mechanism can work even when consistently accounting for gravity darkening, at least for a density contrast up until ten (observed values are on the order of hundred). Curé *et al.* (2005) showed that near critical rotation enables the wind to ‘switch’ from the standard, fast-accelerating solution to a slow, shallow-accelerating velocity law. This, in combination with the bi-stability effect,

can lead to the formation of a slow and dense equatorial wind. Madura *et al.* (2007), finally, confirmed and explained the ‘Curé-effect’, but argued that gravity darkening is still a problem when aiming at a significant density contrast.

4.3. Test beds for the bi-stability jump (II): ‘normal’ B-supergiants

Thus, it is still unclear whether B[e] supergiants can be used to verify the bi-stability effect. Consequently, we now consider ‘normal’ B-supergiants. One of the predictions by Vink *et al.* (2000) is an abrupt decrease of v_∞ (see also Lamers *et al.* 1995) around the bi-stability jump (around 23 kK). Let us first consider this effect. Standard line-driven wind theory predicts that $v_\infty \approx 2.24\alpha/(1-\alpha)v_{\text{esc}}$ (e.g., Puls *et al.* 1996), and a compilation of different measurements/analyses (mostly based on Evans *et al.* 2004 and Crowther *et al.* 2006) by Markova & Puls (2008) shows that the average ratio $v_\infty/v_{\text{esc}} \approx 3.3$ for $T_{\text{eff}} > 23$ kK and $v_\infty/v_{\text{esc}} \approx 1.3$ for $T_{\text{eff}} < 18$ kK, with a *gradual* decrease in between (see also the original work by Evans *et al.* 2004; Crowther *et al.* 2006). Thus, there *is* an effect on v_∞ , but we also have to check the behaviour of the mass-loss rates. Conventionally, this is done by plotting the modified wind-momentum rate, D_{mom} , as a function of the stellar luminosity, since one of the major predictions from radiation driven wind theory is the well-known wind-momentum luminosity relation (WLR, Kudritzki *et al.* 1995),

$$\log D_{\text{mom}} = \log(\dot{M}v_\infty(R_\star/R_\odot)^{1/2}) \approx x \log(L/L_\odot) + \text{offset}(\text{spect. type, metallicity}),$$

where x has a similar dependence as the offset. (Theoretically, $x = (\alpha - \delta)^{-1}$, where $\delta \approx 0.1$ accounts for ionization effects.)

Fig. 6 compares observationally inferred modified wind-momentum rates for OB-supergiants with the predictions from Vink *et al.* (2000) (for details, see Markova & Puls 2008). As pointed out above, the predicted WLR for B-stars lies *above* the one for O-stars (more increase in \dot{M} than decrease in v_∞), whereas the observations show the opposite. The observed O-star rates (triangles, encircled in blue) lie above the predictions, which can be explained by clumping effects (see below), whereas the observed B-star rates for $T_{\text{eff}} < 22$ kK lie well below the predictions and those for $T_{\text{eff}} > 22$ kK just connect the O-star regime and the cooler B-stars. With respect to \dot{M} itself, a careful analysis shows that \dot{M} either decreases in concert with v_∞ (more likely), or at least remains unaffected (less likely). Globally, however, we do not see the predicted increase in \dot{M} , though a certain maximum around the location of the jump might be present (Benaglia *et al.* 2007). Thus, at least below the bi-stability jump there is a severe problem. Either the predicted \dot{M} for cooler objects are too high, or the ‘observed’ (i.e., derived) ones are too low. Accounting for the observed O-star rates, the latter seems unlikely (and the inclusion of clumping would even increase the discrepancy for the B-stars). A way out of the dilemma might be the potential impact of the ‘slow’ wind solution (see above) on BA-supergiants, as suggested by Granada *et al.* (this volume).

4.4. A separate population?

Returning to the problem of the low rotation rates of B-supergiants and accounting for the above dilemma, one has to admit that *if* indeed the mass-loss rates were not increasing at the bi-stability jump, then there would be no bi-stability braking, and the rapid drop of rotation below $T_{\text{eff}} = 20$ kK still needs to be explained. To this end, Vink *et al.* (2010) discuss an alternative *scenario II* (see also Langer, this volume): The cooler, slowly rotating supergiants might form an entirely separate, non core hydrogen-burning population, e.g., they might be products of binary evolution (though this is not generally expected to lead to slowly rotating stars), or they might be post-RSG or blue-loop stars.

Support of this second scenario is the finding that the majority of the cooler objects

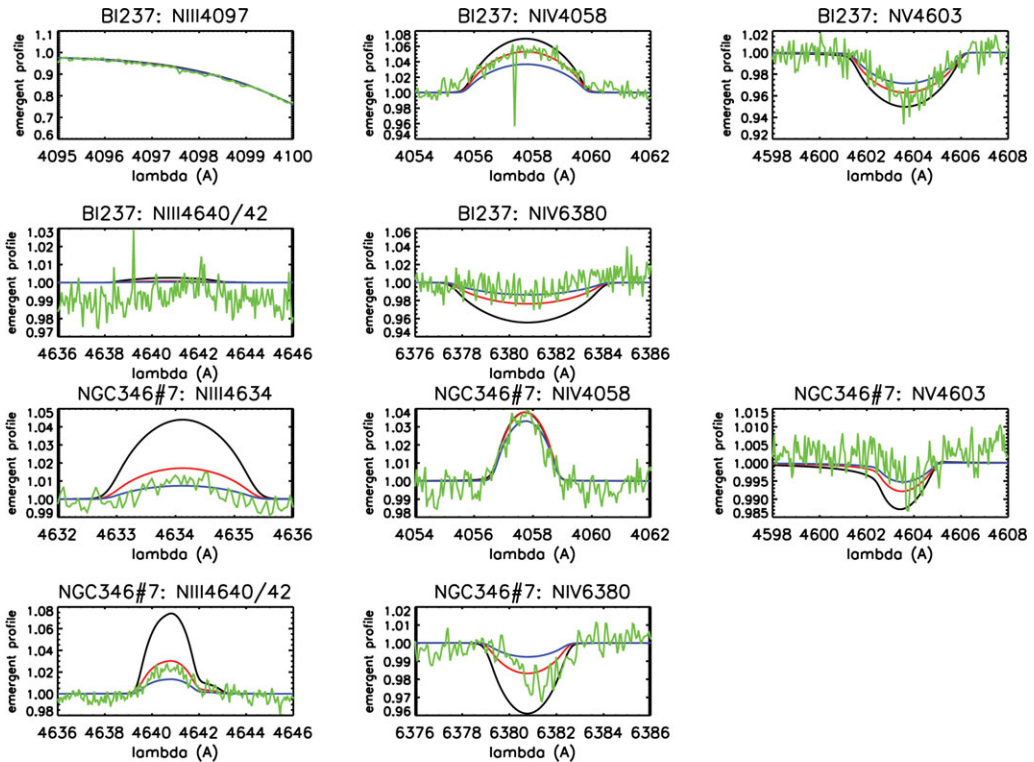


Figure 7. Strategic Nitrogen line profiles in the optical from ionization stages III to V for two early O-type stars. Observations in green, solid lines are synthetic profiles (calculated by the atmospheric code FASTWIND, Puls *et al.* 2005) for different abundances: $N/N_{\odot}=0.2$ (blue), 0.4 (red) and 1.0 (black). Upper panels: BI237 (O2V(f^*)) in the LMC, with $T_{\text{eff}} = 52$ kK and $\log g = 4.0$. The derived Nitrogen abundance is $N/N_{\odot} = 0.4$ or $[N/H] = 7.38$. Lower panels: NGC#7 (O4V(f^+)) in the SMC, with $T_{\text{eff}} = 45$ kK and $\log g = 4.0$. The derived Nitrogen abundance is $N/N_{\odot} \approx 0.2 \dots 0.4$ or $[N/H] \approx 7.08 \dots 7.38$.

(here: in the LMC) is *strongly Nitrogen-enriched*, which was one of the outcomes of the VLT-FLAMES survey of massive stars (Brott, this volume; see also Evans *et al.* 2008 for a brief summary of the project). Vink *et al.* argue that “although rotating models can in principle account for large N abundances, the fact that such a large number of the cooler objects is found to be N enriched suggests an evolved nature for these stars.”

4.5. Nitrogen abundances from O-stars

So far, Nitrogen abundances could be derived only for a subset of the VLT-FLAMES sample stars, and corresponding data are missing particularly for the most massive and hottest stars. Indeed, when inspecting the available literature for massive stars, one realizes that metallic abundances, in particular of Nitrogen, which is *the key element* to check evolutionary predictions, are scarcely found for O-type stars. The simple reason is that they are difficult to determine, since the formation of N III/IV lines (and lines from similar ions of C and O) is problematic due to the impact of various processes that are absent or negligible at cooler spectral types, e.g., dielectronic recombination, mass-loss, and clumping. Within the VLT-FLAMES project, progress is under way (Rivero-González 2010), and in Fig. 7 we show two examples of N-abundance determinations for two early type O-stars in the LMC and SMC. Though no detailed comparison with evolutionary models has

been made yet, the derived abundances for both objects are consistent, within the error-bars, with the average abundances from corresponding B-type stars of early evolutionary stages, which are $[N/H] = 7.13 \pm 0.29$ for the LMC and $[N/H] = 7.24 \pm 0.31$ for the SMC, respectively (Hunter *et al.* 2009).

4.6. Wind clumping

Mass loss is pivotal for the evolution/fate of massive stars (e.g., the formation of GRBs critically depends on the loss of angular momentum due to mass loss, see Ekström and Langer, this volume), their energy release, and their stellar yields. Thus, reliable mass-loss rates are urgently required (ideally better than a factor of two, Meynet *et al.* 1994). O-star mass-loss rates derived from the optical/radio have been found to be higher than predicted by the widely used mass-loss recipe from Vink *et al.* (2000) (see Fig. 6). The present hypothesis assumes that this discrepancy is due to neglected wind-clumping (small scale density inhomogeneities), originating from the line-driven instability, which results in overestimated mass-loss rates when using recombination-based diagnostics (Puls *et al.* 2008, and references therein). To check and infer the effects due to optically thin and thick clumps, and due to porosity in velocity space, on the various diagnostics, Sundqvist *et al.* (2010, 2011) have used the well observed star λ Cep (O6I) as a **test bed** to derive a mass-loss rate of $1.5 \cdot 10^{-6} M_{\odot}/\text{yr}$. This is a factor of four lower than corresponding ‘unclumped’ values and a factor of two lower than the predictions by Vink *et al.* (2000).

5. Very brief summary and conclusions

We discussed OB-stars as extreme condition **test beds**, regarding effects due to pulsations, rapid rotation, and mass-loss. Rapidly rotating B-supergiants (though scarce) are particularly well suited to check a number of theoretical predictions, and the B1 supergiant γ Ara may be a prime candidate for future diagnostics.

Acknowledgements

The authors gratefully acknowledge a travel grant from the IAU and the local organizers of this conference (J.P.), a grant from the IMPRS, Garching (J.O.S.), and a research grant from the German DFG (J.G.R.G.).

References

- Aerts, C., Puls, J., Godart, M., & Dupret, M.-A. 2009, *A&A* 508, 409
 Aerts, C., Lefever, K., Baglin, A., Degroote, P. *et al.* 2010, *A&A* (Letters), 513, L11
 Benaglia, P., Vink, J. S., Martí, J., Maíz Apellániz, J. *et al.* 2007, *A&A* 467, 1265
 Bouret, J.-C., Lanz, T., & Hillier, D. J. 2005, *A&A* 438, 301
 Castor, J. I., Abbott, D. C., & Klein, R. I. 1975, *ApJ*, 195, 157
 Cranmer, S. R. & Owocki, S. P. 1995, *ApJ*, 440, 308
 Crowther, P. A., Lennon, D. J., & Walborn, N. R. 2006, *A&A*, 446, 279
 Curé, M., Rial, D. F., & Cidale, L. 2005, *A&A*, 437, 929
 Domiciano de Souza, A., Kervella, P., Jankov, S., Abe, L. *et al.* 2003, *A&A* (Letters), 407, L47
 Evans, C. J., Lennon, D. J., Trundle, C., Heap, S. R. *et al.* 2004, *ApJ*, 607, 451
 Evans, C., Hunter, I., Smartt, S., Lennon, D. *et al.* 2008, *The Messenger*, 131, 25
 Feldmeier, A., Kudritzki, R.-P., Palsa, R., Pauldrach, A. W. A. *et al.* 1997, *A&A*, 320, 899
 Feldmeier, A., Puls, J., & Pauldrach, A. W. A. 1997, *A&A*, 322, 878
 Fullerton, A. W., Gies, D. R., & Bolton, C. T. 1996, *ApJS*, 103, 475
 Georgiev, L. N., Hillier, D. J., & Zsargó, J. 2006, *A&A*, 458, 597
 Glatzel, W. 1998, *A&A* (Letters), 339, L5
 Howarth, I. D., Siebert, K. W., Hussain, G. A. J., & Prinja, R. K. 1997, *MNRAS*, 284, 265

- Hunter, I., Brott, I., Langer, N., Lennon, D. J. *et al.* 2009, *A&A*, 496, 841
- Kaufer, A., Stahl, O., Prinja, R. K., & Witherick, D. 2006, *A&A*, 447, 325
- Kudritzki, R.-P., Lennon, D. J., & Puls, J. 1995, in: J.R. Walsh & I.J. Danziger (eds.), *Science with the VLT*, Proc. ESO Workshop (Berlin: Springer), p. 246
- Kervella, P. & Domiciano de Souza, A. 2006, *A&A*, 453, 1059
- Lamers, H. J. G. & Pauldrach, A. W. A. 1991, *A&A* (Letters), 244, L5
- Lamers, H. J. G. L. M., Snow, T. P., & Lindholm, D. M. 1995, *ApJ*, 455, 269
- Langer, N., Heger, A., & Fliegner, J. 1997, in: T. R. Bedding, A. J. Booth, & J. Davis (eds.), *Fundamental stellar properties: The interaction between observation and theory*, IAU Symposium 189, p. 343
- Lefever, K., Puls, J., & Aerts, C. 2007, *A&A*, 463, 1093
- Maeder, A. 1999, *A&A*, 347, 185
- Maeder, A. & Meynet, G. 2000, *A&A*, 361, 159
- Madura, T. I., Owocki, S. P., & Feldmeier, A. 2007, *ApJ*, 660, 687
- Markova, N. & Puls, J. 2008, *A&A*, 478, 823
- Massa, D., Fullerton, A. W., Nichols, J. S., Owocki, S. P. *et al.* 1995, *ApJ* (Letters) 452, L53
- Meilland, A., Stee, P., Vannier, M., Millour, F. *et al.* 2007, *A&A* 464, 59
- Meynet, G., Maeder, A., Schaller, G., Schaerer, D. *et al.* 1994, *A&AS*, 103, 97
- Owocki, S. P., Cranmer, S. R., & Gayley, K. G. 1998, in: A. M. Hubert & C. Jaschek (eds.), *B[e] stars*, Astrophysics and Space Science Library 233, p. 205
- Pamyatnykh, A. A. 1999, *AcA*, 49, 119
- Pauldrach, A. W. A. & Puls, J. 1990, *A&A*, 237, 409
- Pelupessy, I., Lamers, H. J. G. L. M., & Vink, J. S. 2000, *A&A*, 359, 695
- Petrenz, P. & Puls, J. 1996, *A&A*, 312, 195
- Petrenz, P. & Puls, J. 2000, *A&A*, 358, 956
- Prinja, R. K., Massa, D., Fullerton, A. W., Howarth, I. D. *et al.* 1997, *A&A*, 318, 157
- Puls, J., Kudritzki, R.-P., Herrero, A., Pauldrach, A. W. A. *et al.* 1996, *A&A*, 305, 171
- Puls, J., Springmann, U. & Lennon, M. 2000, *A&AS*, 141, 23
- Puls, J., Urbaneja, M. A., Venero, R., Repolust, T. *et al.* 2005, *A&A*, 435, 669
- Puls, J., Markova, N., Scuderi, S., Stanghellini, C. *et al.* 2006, *A&A*, 454, 625
- Puls, J., Vink, J. S., & Najarro, F. 2008, *A&AR*, 16, 209
- Repolust, T., Puls, J., & Herrero, A. 2004, *A&A*, 415, 349
- Rivero-González, J. 2010, *Diploma-Thesis* (LMU München)
- Saio, H., Kuschnig, R., Gautschy, A., Cameron, C. *et al.* 2006, *ApJ*, 650, 1111
- Simón-Díaz, S., Herrero, A., Uytterhoeven, K., Castro, N. *et al.* 2010, *ApJ* (Letters) 720, 174
- Sundqvist, J. O., Puls, J., & Feldmeier, A. 2010, *A&A*, 510A, 11
- Sundqvist, J. O., Puls, J., Owocki, S., *et al.* 2011, in: P. Williams & G. Rauw (eds.), *The multi-wavelength view of Hot, Massive Stars*, 39th Liège International Astrophysical Colloquium, in press
- van Belle, G. T. 2010, in: T. Rivinius & M. Curé (eds.), *The Interferometric View on Hot Stars*, Rev. Mexicana AyA Conference Series 38, p. 119
- von Zeipel, H. 1924, *MNRAS*, 84, 665
- Vink, J. S., de Koter, A., & Lamers, H. J. G. L. M. 2000, *A&A*, 362, 295
- Vink, J. S., de Koter, A., & Lamers, H. J. G. L. M. 2001, *A&A*, 369, 574
- Vink, J. S., Davies, B., Harries, T. J., Oudmaijer, R. D. *et al.* 2009, *A&A*, 505, 743
- Vink, J. S., Brott, I., Gräfenor, G., Langer, N. *et al.* 2010, *A&A* (Letters), 512, L7
- Waelkens, C., Aerts, C., Kestens, E., Grenon, M. *et al.* 1998, *A&A*, 330, 215
- Wende, S., Glatzel, W., & Schuh, S. 2008, in: A. Werner & T. Rauch (eds.), *Hydrogen-Deficient Stars*, ASP-CS 391, p. 319
- Zahn, J.-P. 1992, *A&A*, 265, 115
- Zickgraf, F.-J., Wolf, B., Leitherer, C., Appenzeller, I. *et al.* 1986, *A&A*, 163, 119
- Zickgraf, F.-J., Wolf, B., Stahl, O., & Humphreys, R. M. 1989, *A&A*, 220, 206